Controlled transdermal drug delivery using a wireless magnetic microneedle patch: preclinical device development

V. R. Jayaneththi[a*], K. Aw[a], M. Sharma[b], J. Wen[b], D. Svirskis[b], A. J. McDaid[a]

[a]The Department of Mechanical Engineering, Faculty of Engineering, The University of Auckland, Auckland, 1010, New Zealand

[b]School of Pharmacy, Faculty of Medical and Health Sciences, The University of Auckland, Auckland, 1142, New Zealand

*Corresponding author: v.jayaneththi@auckland.ac.nz

Abstract

This paper presents a magnetic polymer-driven transdermal drug delivery system. Transdermal drug delivery has several advantages over oral and hypodermic administration, including painless delivery and avoiding first-pass metabolism. In this study, magnetic polymer composites (MPCs) and inductive sensing principles were utilized as the key actuator and sensor technologies to enable controlled drug release through a single hollow microneedle. The proposed system is capable of drug dispensing and dosage sensing, without the need for on-board electronics or batteries. Through experimental testing, the battery-less device demonstrated controllable zero-order and pulsatile drug release profiles, and was able to pierce and inject solution into excised human skin. This novel wireless pumping system provides the capability to control the volume dispensed for transdermal delivery in a compact, wearable form factor.

Keywords: Transdermal drug delivery; Hollow microneedle; Magnetic polymer; Controlled release; Inductive sensor; Battery-less

1. Introduction

Transdermal drug delivery addresses several major limitations associated with oral and hypodermic delivery routes [1,2]. Transdermal administration delivers compounds to the epidermis, through the outermost layer of skin, the stratum corneum (SC). The SC is the main physical barrier for drug transport through the skin. Compared to intramuscular and subcutaneous hypodermic injections, transdermal delivery is relatively painless and easy to self-administer. Risks of needle-stick injury are avoided and disease transmittance is less likely as the protective function of the skin is less compromised. Compared to oral administration, transdermal delivery avoids hepatic first-pass and digestive metabolic effects, resulting in improved bioavailability and efficacy of the drug in use.

In 1979, the first FDA-approved transdermal product, a scopolamine patch to treat motion sickness, was approved [3]. These early transdermal delivery products relied on slow diffusive properties of drug compounds to penetrate the SC. Because of this, much of the focus, at the time, was on developing low molecular weight (< 500 Da) and balanced lipophilic-hydrophilic formulations [4]. Today, absorption rates can be increased drastically, primarily due to the use of external driving forces, such as ultrasound and iontophoresis [5,6]. However, many formulations used for oral and hypodermic administration have yet to be adapted for the transdermal route simply because they are too large to diffuse through the SC. The rise of microneedle technology has now presented a workaround [7–13]. By piercing the skin, microneedles offer a route that bypasses the SC altogether.

Microneedles are a fraction of the size of traditional hypodermic needles, ranging from hundreds of microns to one millimeter in length. Due to their relatively short lengths, pain-free therapy is possible because dermal nerve endings are avoided [14,15]. Microneedles are either solid or hollow, and can be utilized individually or in an array. Solid needles are typically doped or coated with a drug that is absorbed into the body through dissolution [16,17]. Hollow microneedles instead form a conduit in the SC to deliver compounds directly to the dermal layers. Interestingly, varied flow rates (e.g. bolus, infusion or pulsatile flow) can be achieved by simply controlling the applied pressure [18]. As the pharmaceutical industry moves more towards personalized healthcare, the focus is now shifting to wearable systems with all-in-one diagnosis and delivery capabilities [19,20]. With variable delivery

rates, hollow microneedles show promise for applications where on-demand, controlled drug delivery is sought after.

Controllable drug release via the transdermal route is still in its infancy. The maturation of such technology is touted to make way for a new generation of drug delivery devices [20]. Although speculative, this next generation may result in the development of new therapeutic treatment programs and novel drug compounds. Potential treatments that could take advantage of this technology (i.e. rapid delivery and programmable dosage) include, for example, nicotine replacement therapy and local anesthetic for pain relief. In these applications, not only is it important to deliver the correct dose, but a strategy should be in place to adjust dosage according to patient needs. Ideally, a full day of treatment, or longer, should be supplied by a single device or patch [21]. The technology miniaturization trend is driving device development towards this smaller, idealized form factor, with built in functional sensors and actuators. Transdermal systems (e.g. patches), however, are designed for single use only, making them synonymous with disposability [22]. Decreasing costs by avoiding design complexity (e.g. motors, electronics etc.) is necessary if this technology is to be deployed at scale [23].

Magnetic polymer composites (MPCs) are magnetically driven, shape changing materials capable of fast, wireless actuation [24–26]. This material actuator is composed of an elastomeric matrix with embedded magnetic microparticles. Material deformation is induced when an external magnetic field is applied. The key advantage of this smart material is that it does not require "on-board" circuitry to operate, making it ideal for wireless, battery-less applications. Existing applications of MPC include microfluidics [27], artificial muscle [28] and implantable drug delivery microrobots [29]. Here, MPC is a promising smart material that can be applied to achieve controllable drug delivery while also reducing design complexity.

In this paper, a new transdermal drug delivery system, capable of on-demand, controllable drug release is presented. With no active components inside the patch-like device, the proposed system is capable of wireless actuation and dosage sensing. A volume displacement pump, developed using MPC, was used to drive fluid through a single hollow microneedle. Polymeric microneedles are commonly described in literature, however, they are brittle and prone to degradation [30]. In this work, durable stainless-

steel microneedles were manufactured and utilized. Furthermore, to track dosage and drug dispensed, an inductive sensing approach to wirelessly sense reservoir volume is described herein.

The main contribution of this work is the development of a battery-less transdermal drug delivery device that can achieve active on-demand dosing and volume sensing. The proposed system provides a novel method to control the dosage dispensed for transdermal drug delivery. By excluding "on-board" electronics and reducing design complexity, the device was inherently developed with disposability in mind i.e. for single-use applications. The specific objectives of this study were to characterize the performance of the MPC pump, validate the reservoir volume sensor, and demonstrate controllable drug release. *Ex vivo* experiments were also conducted to determine if the device can pierce the SC and inject formulation into the dermal layers of excised human skin.

2. Materials and Methods

2.1 Device Working Principles

Figure 1 illustrates how the device is actuated and how drug is delivered. The built-in MPC-driven volume displacement pump operates when exposed to an external magnetic field. When the field is briefly switched on, i.e. pulsed, the MPC diaphragm is displaced towards the magnetic source. As the volume inside the pump chamber decreases, pressure increases. When the cracking pressure of the outlet check valve is overcome, air is forced into a secondary chamber. Pressure in this secondary chamber exerts an increasing force on the drug reservoir, thus driving fluid flow through the hollow microneedle. When the magnetic field is removed, the elastic restoring force of the MPC diaphragm generates a negative chamber pressure that brings in air and refills the pump. Here, the magnetic field was generated by a pulse coil system (MP6, SOTA Instruments, Canada) capable of producing high field strengths. The strength and duration of each magnetic pulse was 0.6 T and 2.5 milliseconds, respectively. A strong magnetic field was required to generate sufficient pump pressure to overcome the check valve's cracking pressure (~4 kPa). Micro check valves (Ø2.5 mm, The Lee Company, USA) were installed at the inlet and outlet of the MPC pump to ensure one-way airflow during operation. Note, these check
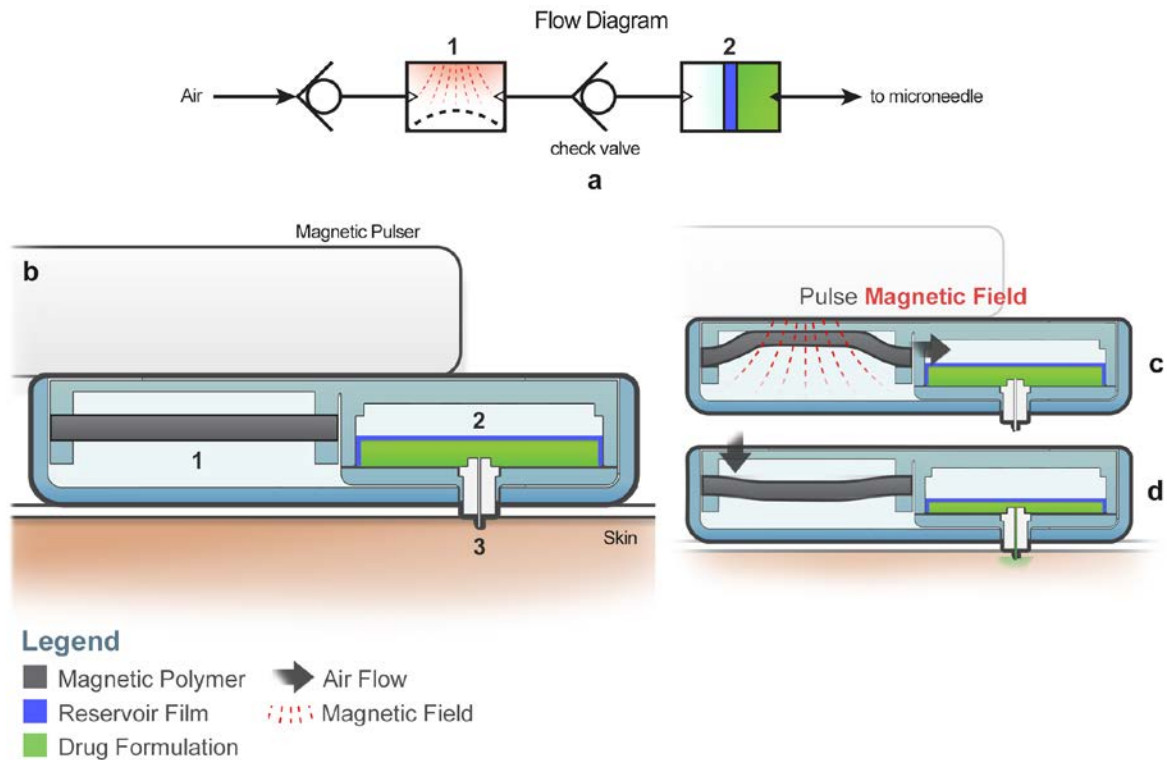
Figure 1. a) Process flow diagram of the overall pneumatic-hydraulic actuator system. b) The simplified cross section of the device (e.g. check valves, seal omitted for clarity); the MPC volume displacement pump (1) and drug reservoir (2) are pictured. The device has a single hollow microneedle (3) that pierces the top layer of skin to bypass the stratum corneum. c) The MPC pump displaces air into the secondary chamber when the magnetic field is pulsed. Check valves are present to ensure air flows in only one direction. d) Fluid flow is driven by the pressure increase in the secondary chamber. Drug formulation is injected into the dermal layers via the microneedle and is absorbed into systemic circulation by neighbouring capillaries. The elastic restoring force of the MPC diaphragm refills the magnetic pump with air.

valves were not affected by magnetic fields because they were manufactured from austenitic stainless steel.

For controlled drug release, a closed loop feedback system is required for accurate dosing. Inductive sensing provides a novel method to wirelessly sense the amount of drug released by the device. The principles of inductive sensing are as follows. A high frequency alternating current is applied to a detector coil. This generates an oscillating magnetic field that can be indirectly measured by determining the effective inductance of the coupled system. When a conductive element is brought near the oscillating field, eddy currents are induced on its surface, which in turn produce their own magnetic field. The interaction between the two fields (i.e. detector and conductive element) result in a measurable change in inductance. The magnitude of this change is dependent on the distance between
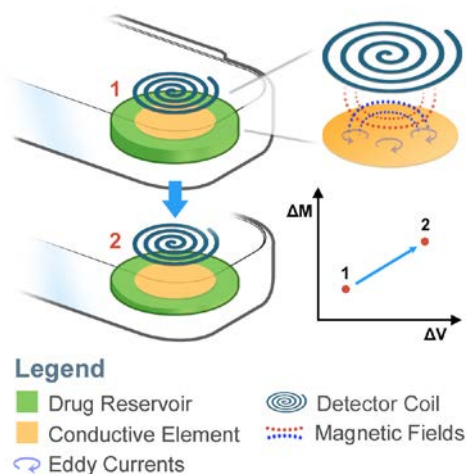
Figure 2. Inductive sensing principles were applied to wirelessly measure volume dispensed. The oscillating magnetic field from the planar detector coil (placed externally) induces eddy currents in the conductive element. These eddy currents produce their own magnetic field. The interaction between the two fields results in a change in inductance (ΔM) which can be used to determine the change in volume (ΔV).

the detector coil and conductive element. In this work, inductive sensing was applied to wirelessly sense the total volume dispensed, or released, by the drug delivery device.

The implementation of the volume sensor is outlined in Figure 2. Here, the conductive element, a thin copper film, was attached to the drug reservoir. The diameter and thickness of the copper film were 12.5 mm and 80 µm, respectively. For sensing, a two-layered planar detector coil was placed on top of the device, centrally aligned with the axis of the copper film. The diameter and turns per layer for this coil were 13.9 mm and 19, respectively. The track width and spacing were both 0.15 mm.

As the pressure builds up in the secondary chamber and drug exits the device, the copper film is displaced. This displacement affects the interaction between the induced and applied oscillating fields. The resulting change in inductance of the system (and thereby volume dispensed) was measured using an external sensor module (LDC1614EVM, Texas Instruments, USA) interfaced to the detector coil.

2.2 Device Fabrication

An overview of the assembled device is provided in Figure 3. The final dimensions of the patch-like device were 53.1 x 30.0 x 11.3 mm. The dry weight of the device was 12 g. The internal drug reservoir is a flexible polyethylene pouch that can hold 0.5 ml of solution. This reservoir is filled via the
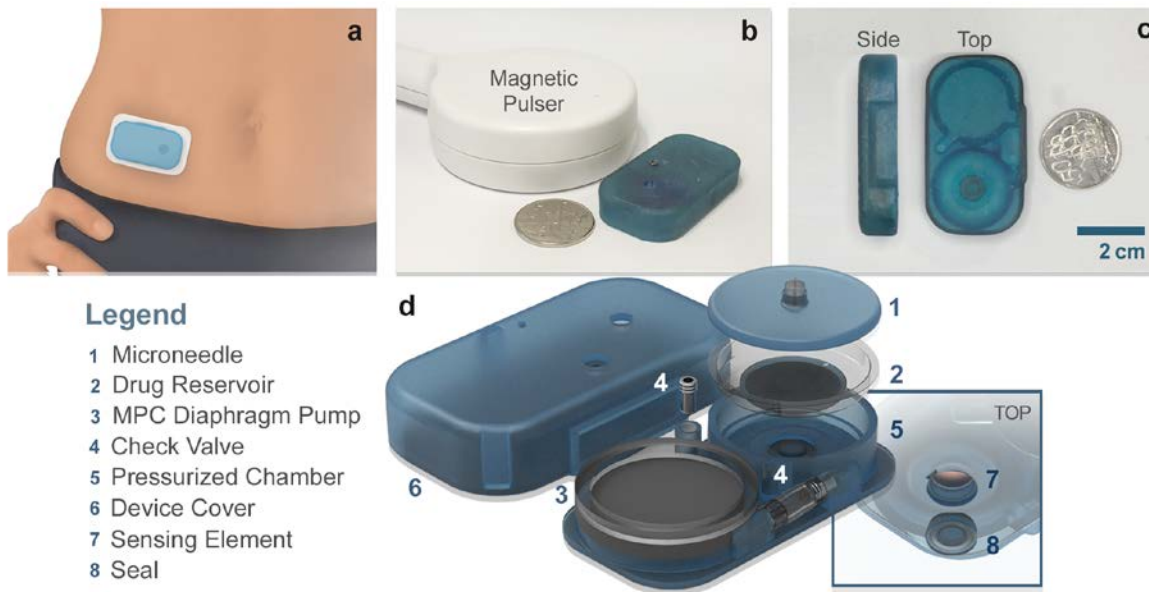
Figure 3. a) The proposed device is a battery-less wearable capable of delivering drug formulation directly into the dermal layers of skin, b) Photo of the assembled device and handheld magnetic pulser (New Zealand 50 cent coin for scale), c) Photo of the side and top of the assembled device, d) Exploded view of the device assembly; the check valves (4) are located at the inlet and outlet of the MPC pump (3).

microneedle; the top seal is removed during this process to equalize pressure in the secondary chamber with the atmosphere. Attached to the underside of the drug reservoir is the copper film used for inductive sensing. The device (chambers and air flow channels) were printed as a single component using stereolithographic 3D printing (Tough Resin, Formlabs, USA). Plastic adhesive was used to seal components together (All Plastics Superglue, Loctite, Germany).

2.2.1 MPC Diaphragm Fabrication

MPCs consist of two components; an elastomer and magnetic filler. Here, silicone was used for the elastomeric matrix (Ecoflex 00-30, Smooth-On, USA). The magnetic filler was atomized iron powder (Inoxia Ltd, UK). To begin, the two constituents were thoroughly mixed together using a planetary mixer (Mazerustar KK-50S, Kurabo, Japan). The loading of the magnetic filler was 30% w/w. Note, the silicone elastomer was a liquid solution prior to polymerization. The uncured solution was then cast into a 60 mm diameter mold, 2.5 mm thick. The sample was placed in a temperature-controlled oven and left to cure for one hour at 80 °C. Once cured, a circular MPC diaphragm was cut out and pre-strained to 10% to provide the aforementioned elastic restoring force for the MPC pump. The diameter of the pre-strained diaphragm was 25 mm.
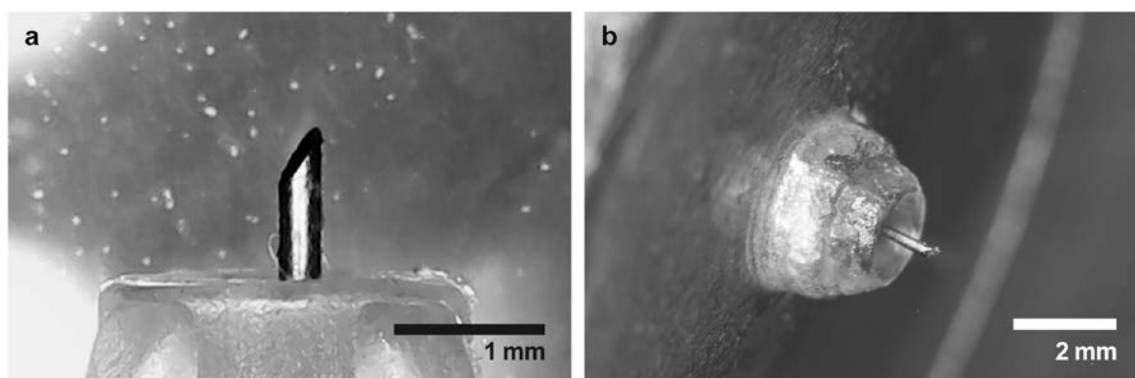
2.2.2 Microneedle Fabrication

Figure 4. A single microneedle was used to inject formulation into skin. Femtosecond laser micromachining was used to fabricate the microneedle. The outer diameter, bore diameter and length were 235, 108 and 1000 µm, respectively. The bevel angle was 60º. a) Close-up image of the microneedle, b) microneedle in the assembled device (shown with device cover taken off).

Stainless-steel microneedles were fabricated in house because hollow microneedles were not yet commercially available. The machined microneedles are presented in Figure 4. Starting with an off-the-shelf 32G needle (Micro-Fine™, Becton Dickinson, USA), the desired microneedle geometry was manufactured using femtosecond laser micromachining. The outer diameter, bore diameter and length of the microneedles were 235, 108 and 1000 µm, respectively. A beveled tip angle of 60º was chosen to reduce the force required for SC penetration and enhance needle durability [31]. Note, the proposed device only utilized a single microneedle.

2.3 Volume Sensor Calibration

The volume sensor must be calibrated by establishing the relationship between change in inductance and volume dispensed. To be clear, the sensor measures the volume of drug dispensed, or released, by the device, not drug delivered into the body. This sensor was calibrated through experimentation. Volume dispensed was determined by measuring the mass of the injected solution using a precision mass balance (CP323S, Sartorius AG, Germany). To begin, the drug reservoir was filled with solution (deionized water). The density of deionized water was assumed to be 0.9982 g/cm^3 at 20 °C. The planar detector coil was placed on top of the device and the inductance was measured as solution was dispensed onto the mass balance. Care was taken to ensure the mass balance was not affected by the magnetic
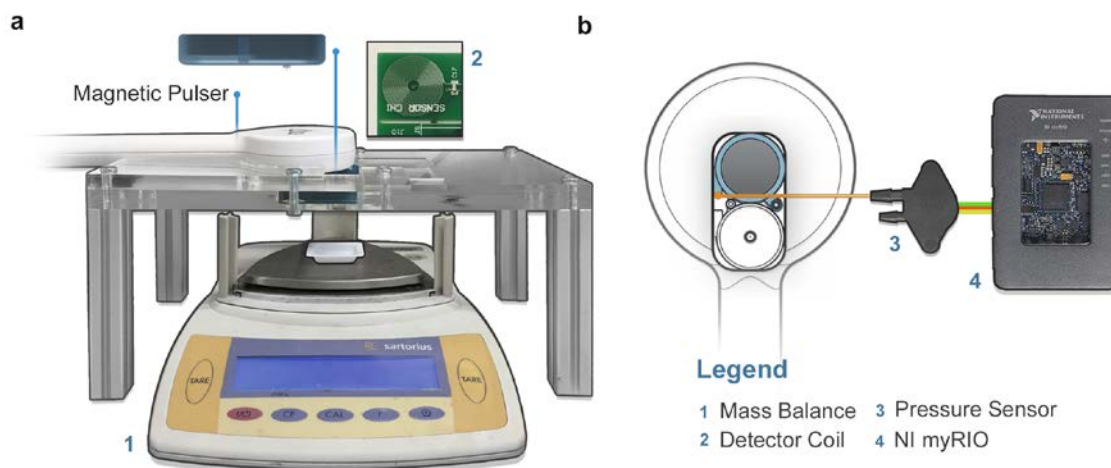
Figure 5. a) The experimental setup to calibrate the wireless volume sensor. The same setup was used to measure drug release kinetics. The device was loaded with solution and placed above a precision mass balance. As the magnetic field was pulsed, fluid flow was measured by recording change in mass. A photograph of the planar detector coil is also pictured (a separate component and not integrated in the magnetic pulser). b) Experimental setup for pressure testing. The outlet of the MPC pump was interfaced to a differential pressure sensor. The other end of the pressure sensor was exposed to atmospheric pressure. Pressure measurements were recorded using a National Instruments myRIO. The MPC pump was positioned at the centre of the magnetic pulser i.e. where the field is the strongest. A check valve was placed in series with the pressure sensor to measure sustained pressure.

field i.e. distance between the pulser and the balance was set to ~180 mm to negate any interaction. All experiments were repeated three times. The experimental setup is highlighted in Figure 5 (a).

2.4 MPC Pump Performance

MPC pump performance can be quantified by measuring back pressure; the pressure generated at the outlet of a pump, and the sustained pressure when the check valve is present. In this case, sustained pressure is indicative of the flow rates that can be achieved during drug delivery. A differential pressure sensor (MPX5050DP, NXP USA Inc., USA) was connected to the outlet of the MPC pump, illustrated in Figure 5 (b). The maximum back pressure generated by the pump was first measured, followed by the maximum sustained pressure i.e. with check valve in place. The maximum sustained pressure was determined by pulsing the device several times. Pressure measurements were recorded using a real-time data acquisition interface (myRIO, National Instruments, USA). All experiments were repeated three times.

2.5 *Ex Vivo* Tissue Injection

Ex vivo experiments were carried out to determine if the device can pierce the stratum corneum and deliver drug to the dermal layers of excised human skin. Skin samples were obtained from breast reduction surgery with the approval of the University of Auckland Human Participants Ethics Committee (Ref: 010990). Subcutaneous fat was carefully removed using a scalpel. Once processed, the skin was wrapped in aluminum foil and stored at -20 °C.

Before the experiment, frozen skin samples were defrosted for 30 minutes at room temperature. Sample size was approximately 10 x 10 mm. The outer surface of the skin was gently wiped with a PBS-soaked cotton pad before it was loaded onto a polystyrene cube [32,33]. The cube provided support during piercing. The drug reservoir was loaded with 0.05% w/v crystal violet (Chem-Supply, Australia) to stain the tissue for improved visualization. To begin, the drug delivery device was placed on top of the magnetic pulser. Holding the skin sample, a gentle downward force was applied on the polystyrene cube to ensure the microneedle pierced the SC. The device was then pulsed several times. The skin sample was removed and refrozen for imaging.

2.6 Drug Release Kinetics

Unlike diffusion-driven transdermal systems, this device provides control over the drug delivery rate. Delivery rate is controlled by varying the pressure acting on the reservoir, which, in this case, is achieved by changing the pulse frequency i.e. the time between consecutive magnetic pulses. As fluid exits the device, pressure decreases. To maintain a high flow rate, a high pulse frequency is required, vice versa.

Three different magnetic pulsing strategies were employed to demonstrate on-demand, controllable drug release; fast continuous, slow continuous and fast pulsatile [34]. Volume dispensed was measured over time to show that drug release rate can be controlled. The pulse frequency for the fast and slow release profiles were 0.17 and 0.017 Hz, respectively. For pulsatile release, the pulse frequency was set to 0.17 Hz with intermittent breaks every 150 seconds, lasting 150 seconds each. The experimental setup is the same as that outlined in Figure 5 (a). The total duration of each experiment was 10 minutes. All three experiments were repeated three times.
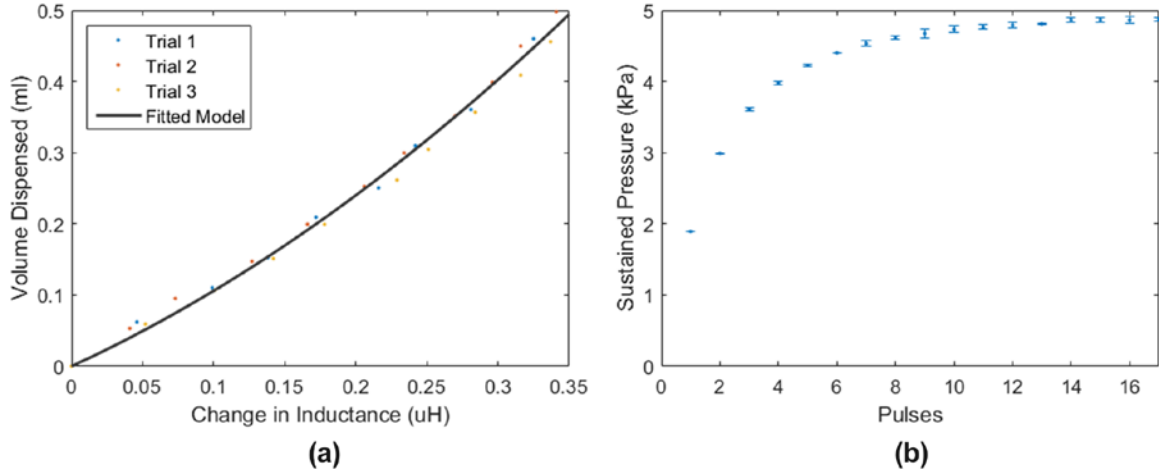
Figure 6. (a) Volume dispensed by the device vs change in inductance. The RMS error between the fitted model and experimental data was 0.012 ml. This model was used to wirelessly determine the total volume of drug dispensed. (b) Sustained pressure vs magnetic pulses. The maximum sustained pressure was 4.87 ± 0.031 kPa. Six pulses were required to reach 90% of this maximum. Note, mean and standard deviation were plotted at each point.

3. Results

3.1 Volume Sensor Calibration

The relationship between the change in inductance and volume dispensed is illustrated in Figure 6 (a). A second-order polynomial model was fitted to the data using linear least-squares regression, and is expressed by the following equation,

$$V = aM^2 + bM \qquad (1)$$

$$a = 1.41, b = 0.92$$

Where, V is the volume dispensed (ml), M is the effective change in inductance of the system (µH) and a, b are the fitted model constants. The root mean square (RMS) error between the fitted model and experimental data was 0.012 ml. These results highlight the repeatability and accuracy of the applied inductive wireless sensing approach.

3.2 MPC Pump Performance

The mean maximum back pressure for the MPC pump was 5.68 ± 0.074 kPa. The sustained pressure results are presented in Figure 6 (b). The maximum mean sustained pressure was 4.87 ± 0.031 kPa, with
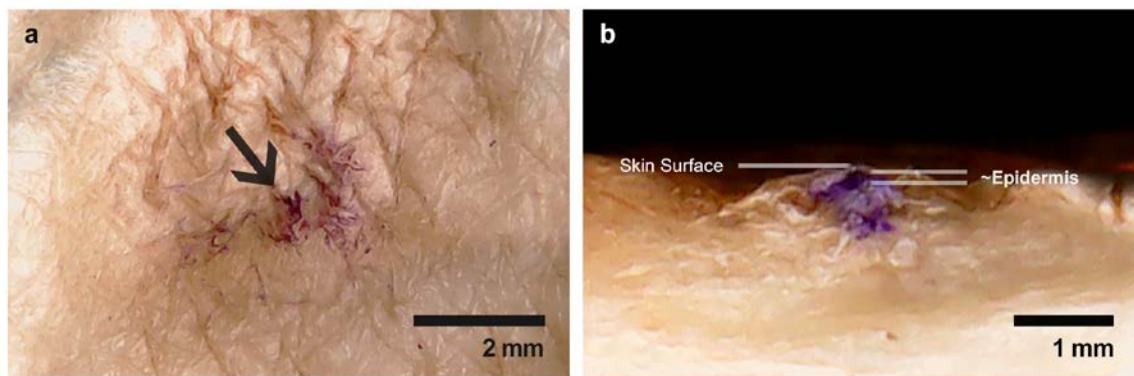
Figure 7. a) Top view of the injection site on excised skin. The arrow indicates the location where the needle pierced the stratum corneum. b) Cross section of the injection site. The mock drug formulation (crystal violet stain) has clearly reached the dermal layers of the skin. The skin surface and epidermis are labelled for reference.

six pulses required to reach 90% of this maximum. The difference between the maximum back pressure and sustained pressure was due to losses in the system, e.g. overcoming check valve cracking pressure and fluid frictional losses.

3.3 Excised Skin Injection

The machined microneedle and MPC pump demonstrated the capability to pierce the SC and deliver drug into the dermal layers. Microscope images of the top and cross section of the injection site are presented in Figure 7. Note, the thickness of the human skin sample was 2.6 mm.

3.4 Drug Release Profiles

The experimental drug release profiles are presented in Figure 8. The mean volume dispensed versus time for each delivery strategy is plotted. The mean ($\pm$SD) flow rate for the fast and slow continuous release profiles were relatively constant (i.e. zero-order) at 108 (2.6) µL/min and 9.07 (0.28) µL/min, respectively. The drug reservoir (0.5 ml) was emptied in approximately 330 seconds with the fast pulsing strategy. The mean ($\pm$SD) flow rate for the fast pulsatile release profile, during each pulsing sequence, was also consistent at 105 (2.1) µL/min and 103 (8.3) µL/min, respectively. These results confirm on-demand, controllable drug release is possible with the proposed battery-less system.
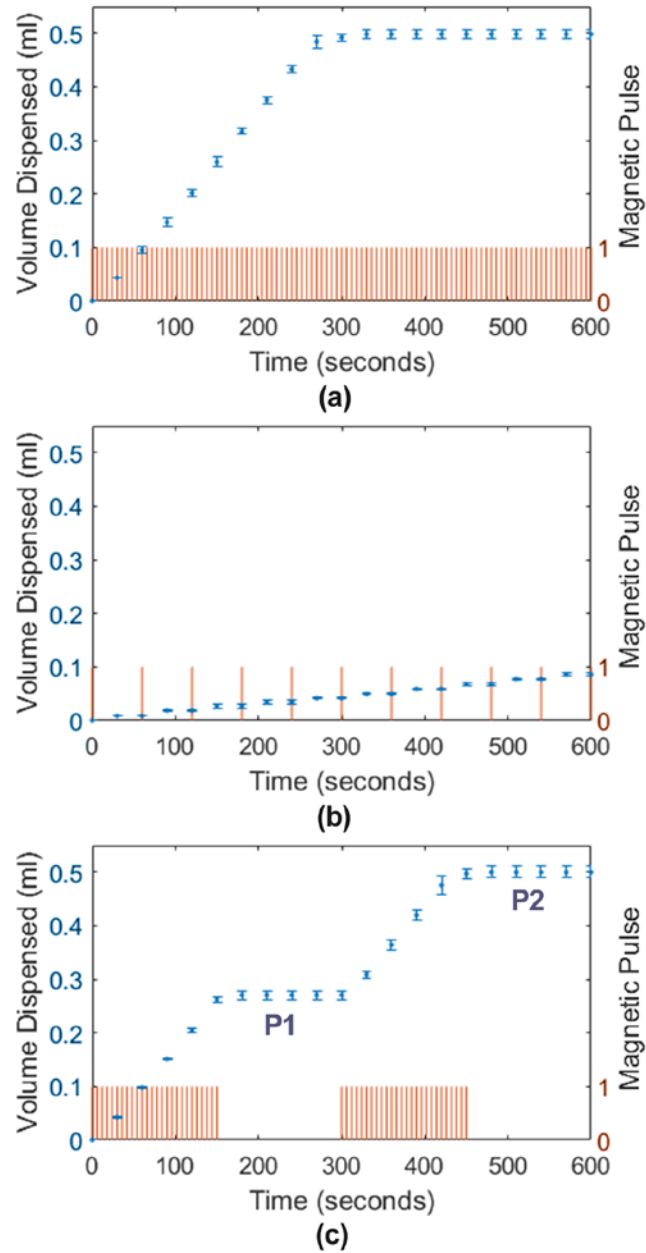
3.5 Volume Sensor Validation

Figure 8. Experimental drug release profiles. Three pulsing strategies were employed to achieve different release profiles: (a) fast continuous, (b) slow continuous and (c) fast pulsatile. Note, the device can hold up to 0.5 ml. The release profiles were achieved by simply varying the timing between subsequent magnetic pulses, highlighted in red, where 1 indicates a pulse. P1 and P2 indicate the intermittent breaks during pulsatile release. Note, the mean and standard deviation of volume dispensed is plotted at each point.

To validate the wireless volume sensor, sensor readings were recorded at the midpoint of each intermittent break during pulsatile release (P1, P2). These readings were compared against the actual volume dispensed (measured using the mass balance). The mean absolute percentage (±SD) error at

each plateau, P1 and P2, was 4.9% (1.5) and 3.3% (1.9), respectively. This low error provides further confirmation that accurate volume sensing can be achieved with the applied wireless approach.

4. Discussion

This paper presented a transdermal drug delivery system capable of on-demand, controlled release. The single microneedle system bypasses the SC and injects formulation directly into dermal tissue. Unlike traditional transdermal patches, which rely on diffusion-based processes, this device provides a viable route to deliver drug molecules with high molecular weight and poor penetrating properties. Other therapeutic advantages include enhanced delivery rates (due to the microneedle and active driving force provided by the MPC pump) [35] and variable dosing. For the pediatric population, or those with needle phobia, the microneedle device also provides a relatively pain-free means of drug delivery that may lead to improved patient compliance [36,37]. Given the volume of the reservoir (0.5 ml), the device would be most useful for concentrated solutions of potent drugs, however, this would depend on how frequently the device is replaced.

The device achieved wireless actuation and volume (or dosage) sensing without on-board electronics or batteries. Minimizing the number of internal components has allowed the wearable device to be lightweight and have a low profile. The discreet form factor may help eliminate social stigma associated with traditional wearable medical devices and enable easier adoption. From a manufacturing perspective, avoiding electronics altogether also reduces design complexity and costs.

To operate the device, an external handheld electromagnetic pulser was used. This device was connected to the mains power supply, however, the operating principles of magnetic pulsing (i.e. capacitive charging and discharging) lends itself well to further miniaturization and battery-driven operation. For perspective, the energy per pulse for the pulser (i.e. energy stored on the capacitor) was ~37 J. A typical 1.5V AA battery holds approximately 13 kJ of energy; this equates to ~351 pulses or, based on the experimental results presented, ~3.8 ml dispensed before the battery would require replacement.

The efficiency of the system could be improved by optimizing the electromagnet design of the magnetic pulser. Optimizable parameters include coil diameter, coil height, number of windings, wire gage and even morphology [38]. It should be noted that the existing electromagnet design is an air-core solenoid. Therefore, the strength of its magnetic field can be greatly increased by simply adding a ferrous core [39]. Geometrical optimization can also be carried out on the MPC pump using previously established modeling methods [40,41]. However, inefficiencies in the existing pump are mostly due to fluid frictional losses at the outlet. The outlet in the current design features a vertical 90° bend, connecting the pump to the check valve and secondary chamber. This bend was included to minimize the volume of the device packaging. In the current design, the maximum back pressure was 5.75 kPa. However, a modified MPC pump was later tested without this vertical bend and the back pressure was measured to be 12.3 kPa, which demonstrated a significant improvement. With this mind, the arrangement of internal components will be more carefully considered in the next design iteration.

The device demonstrated controllable, zero-order drug release when injecting into air. Resistance due to dermal tissue was not considered. In previous literature, dermal resistance has been of concern for hollow microneedle drug delivery [42–44]. Fortunately, solutions have been proposed to combat potential blocked flow by, for example, slightly retracting the needle after piercing to form a cavity [44–46] or by using hyaluronidase to break down hyaluronic acid in surrounding collagen fibers [43]. It should also be noted that the skin model used for the *ex vivo* experiments does not replicate the *in vivo* environment. Once removed from the body, the natural tautness of human skin is lost. More importantly, the absorptive properties are reduced because functioning capillaries are not present [47]. Despite this, a foundation has been established for a comprehensive *in vivo* study to further investigate the effects of dermal resistance on flow rate, as well as other factors such as the long-term effects of using the device, e.g. inflammation, skin irritation [48].

A single hollow microneedle was utilized in the proposed device. This needle was capable of piercing the stratum corneum and enabling injection into the dermal layers. Another advantage of hollow microneedle technology, not explored here, is microneedle arrays. Arrays offer multiple points of entry, thus increasing the potential injection flow rate [42]. Integrating microneedle arrays should be

investigated in future, although, careful consideration needs to be placed on optimizing the number of needles and their spatial arrangement. Increasing the number of microneedles has shown to increase pain [37].

The efficiency or effectiveness of the drug delivery system was not investigated in this work. This preclinical study established a transdermal delivery system capable of controlling the volume of drug released. However, this does not indicate that the full dose will be delivered and absorbed by the body. This is a limitation of the current study. Other factors (unintentional or not) may affect drug delivery, such as, leaking [12] or improper use. To quantify the effectiveness of the system for controlled drug delivery, *in vivo* trials are required where uncontrolled variables (e.g. skin thickness, sweat, movement) are present. The efficiency of the system could be determined, for example, by measuring blood concentration over the course of each trial. Moving forward, *in vivo* testing on animal models (i.e. porcine) is necessary before conducting clinical trials.

The wireless volume sensor will be important for future *in vivo* studies. Due to variance in tissue composition, drug release rates will vary between individuals. The sensor allows for active feedback control to ensure the correct dose has been dispensed. In the current system, simultaneous pulsing and volume sensing was not possible due to spatial constraints. For real-time dosage control, the next design will integrate the detector coil into the magnetic pulser.

5. Conclusions

In this paper, a novel MPC-driven transdermal drug delivery system was presented. The device was capable of wireless volume sensing and controllable drug release with no "on-board" electronics or power supply. With a single hollow microneedle, the device can deliver compounds directly to the dermal layers of skin and avoid some limitations of traditional transdermal delivery e.g. slow absorption, low molecular weight drugs. Here, magnetic polymer composites (MPCs) and inductive sensing were utilized as the key actuator and sensing technologies to enable wireless controllable dosing.

Following further design optimization, the results presented in this paper have set the foundation to carry out future *in vivo* trials and investigate the effectiveness of the device when delivering bioactive agents in live subjects.

Acknowledgements

References

[1]   Prausnitz MR, Langer R. Transdermal drug delivery. Nat Biotechnol 2008;26:1261–8. doi:10.1038/nbt.1504.

[2]   Watkinson AC, Kearney M-C, Quinn HL, Courtenay AJ, Donnelly RF. Future of the transdermal drug delivery market – have we barely touched the surface? Expert Opin Drug Deliv 2016;13:523–32. doi:10.1517/17425247.2016.1130034.

[3]   Pastore MN, Kalia YN, Horstmann M, Roberts MS. Transdermal patches: history, development and pharmacology. Br J Pharmacol 2015;172:2179–209. doi:10.1111/bph.13059.

[4]   Wiedersberg S, Guy RH. Transdermal drug delivery: 30 + years of war and still fighting! J Control Release 2014;190:150–6. doi:10.1016/J.JCONREL.2014.05.022.

[5]   Barry B. Novel mechanisms and devices to enable successful transdermal drug delivery. Eur J Pharm Sci 2001;14:101–14. doi:10.1016/S0928-0987(01)00167-1.

[6]   Subedi RK, Oh SY, Chun M-K, Choi H-K. Recent advances in transdermal drug delivery. Arch Pharm Res 2010;33:339–51. doi:10.1007/s12272-010-0301-7.

[7]   Indermun S, Luttge R, Choonara YE, Kumar P, du Toit LC, Modi G, et al. Current advances in

the fabrication of microneedles for transdermal delivery. J Control Release 2014;185:130–8. doi:10.1016/J.JCONREL.2014.04.052.

[8]   Bariya SH, Gohel MC, Mehta TA, Sharma OP. Microneedles: an emerging transdermal drug delivery system. J Pharm Pharmacol 2012;64:11–29. doi:10.1111/j.2042-7158.2011.01369.x.

[9]   Cheung K, Das DB. Microneedles for drug delivery: trends and progress. Drug Deliv 2014:1–17. doi:10.3109/10717544.2014.986309.

[10]   Ma G, Wu C. Microneedle, bio-microneedle and bio-inspired microneedle: A review. J Control Release 2017;251:11–23. doi:10.1016/J.JCONREL.2017.02.011.

[11]   Ruggiero F, Vecchione R, Bhowmick S, Coppola G, Coppola S, Esposito E, et al. Electro-drawn polymer microneedle arrays with controlled shape and dimension. Sensors Actuators B Chem 2018;255:1553–60. doi:10.1016/j.snb.2017.08.165.

[12]   Resnik D, Možek M, Pečar B, Janež A, Urbančič V, Iliescu C, et al. In vivo experimental study of noninvasive insulin microinjection through hollow Si Microneedle Array. Micromachines 2018;9. doi:10.3390/mi9010040.

[13]   Golombek S, Pilz M, Steinle H, Kochba E, Levin Y, Lunter D, et al. Intradermal Delivery of Synthetic mRNA Using Hollow Microneedles for Efficient and Rapid Production of Exogenous Proteins in Skin. Mol Ther - Nucleic Acids 2018;11:382–92. doi:10.1016/j.omtn.2018.03.005.

[14]   Prausnitz MR. Microneedles for transdermal drug delivery. Adv Drug Deliv Rev 2004;56:581–7. doi:10.1016/J.ADDR.2003.10.023.

[15]   Kaushik S, Hord AH, Denson DD, McAllister D V., Smitra S, Allen MG, et al. Lack of Pain Associated with Microfabricated Microneedles. Anesth Analg 2001;92:502–4. doi:10.1213/00000539-200102000-00041.

[16]   Gill HS, Prausnitz MR. Coated microneedles for transdermal delivery. J Control Release 2007;117:227–37. doi:10.1016/J.JCONREL.2006.10.017.

[17]   Lee JW, Park J-H, Prausnitz MR. Dissolving microneedles for transdermal drug delivery. Biomaterials 2008;29:2113–24. doi:10.1016/J.BIOMATERIALS.2007.12.048.

[18]   Van Der Maaden K, Jiskoot W, Bouwstra J. Microneedle technologies for (trans)dermal drug and vaccine delivery. J Control Release 2012;161:645–55. doi:10.1016/j.jconrel.2012.01.042.

[19]   Lee H, Song C, Hong YS, Kim MS, Cho HR, Kang T, et al. Wearable/disposable sweat-based glucose monitoring device with multistage transdermal drug delivery module. Sci Adv 2017;3:e1601314. doi:10.1126/sciadv.1601314.

[20]   Lee H, Song C, Baik S, Kim D, Hyeon T, Kim D-H. Device-assisted transdermal drug delivery. Adv Drug Deliv Rev 2018;127:35–45. doi:10.1016/J.ADDR.2017.08.009.

[21]   Stevenson CL, Santini JT, Langer R. Reservoir-based drug delivery systems utilizing microtechnology. Adv Drug Deliv Rev 2012;64:1590–602. doi:10.1016/J.ADDR.2012.02.005.

[22]   Ochoa M, Mousoulis C, Ziaie B. Polymeric microdevices for transdermal and subcutaneous drug delivery. Adv Drug Deliv Rev 2012;64:1603–16. doi:10.1016/j.addr.2012.09.035.

[23]   Kim B, Seong K-Y, You I, Selvaraj V, Yim S-G, O'Cearbhaill ED, et al. Touch-actuated transdermal delivery patch for quantitative skin permeation control. Sensors Actuators B Chem 2018;256:18–26. doi:10.1016/J.SNB.2017.10.059.

[24]   Jayaneththi VR, Aw KC, McDaid AJ. Wireless magnetic polymer actuator for implantable applications. 2017 IEEE Int. Conf. Adv. Intell. Mechatronics, IEEE; 2017, p. 791–6. doi:10.1109/AIM.2017.8014114.

[25]   Nguyen VQ, Ahmed AS, Ramanujan R V. Morphing Soft Magnetic Composites. Adv Mater 2012;24:4041–54. doi:10.1002/adma.201104994.

[26]   Thévenot J, Oliveira H, Sandre O, Lecommandoux S. Magnetic responsive polymer composite materials. Chem Soc Rev 2013;42:7099–116. doi:10.1039/c3cs60058k.

[27]   Li J, Zhang M, Wang L, Li W, Sheng P, Wen W. Design and fabrication of microfluidic mixer

from carbonyl iron - PDMS composite membrane. Microfluid Nanofluidics 2011;10:919–25. doi:10.1007/s10404-010-0712-2.

[28]   Ahmed AS, Ramanujan R V. Hysteretic Buckling for Actuation of Magnet-Polymer Composites. Macromol Chem Phys 2015;216:1594–602. doi:10.1002/macp.201500152.

[29]   Huang H-W, Uslu FE, Katsamba P, Lauga E, Sakar MS, Nelson BJ. Adaptive locomotion of artificial microswimmers. Sci Adv 2019;5:eaau1532. doi:10.1126/sciadv.aau1532.

[30]   Dharadhar S, Majumdar A, Dhoble S, Patravale V. Microneedles for transdermal drug delivery: a systematic review. Drug Dev Ind Pharm 2019;45:188–201. doi:10.1080/03639045.2018.1539497.

[31]   Lee D-S, Li CG, Ihm C, Jung H. A three-dimensional and bevel-angled ultrahigh aspect ratio microneedle for minimally invasive and painless blood sampling. Sensors Actuators B Chem 2018;255:384–90. doi:10.1016/J.SNB.2017.08.030.

[32]   Verbaan FJ, Bal SM, van den Berg DJ, Groenink WHH, Verpoorten H, Lüttge R, et al. Assembled microneedle arrays enhance the transport of compounds varying over a large range of molecular weight across human dermatomed skin. J Control Release 2007;117:238–45. doi:10.1016/J.JCONREL.2006.11.009.

[33]   Badran MM, Kuntsche J, Fahr A. Skin penetration enhancement by a microneedle device (Dermaroller®) in vitro: Dependency on needle size and applied formulation. Eur J Pharm Sci 2009;36:511–23. doi:10.1016/J.EJPS.2008.12.008.

[34]   Sanjay ST, Zhou W, Dou M, Tavakoli H, Ma L, Xu F, et al. Recent advances of controlled drug delivery using microfluidic platforms. Adv Drug Deliv Rev 2018;128:3–28. doi:10.1016/j.addr.2017.09.013.

[35]   Norman JJ, Brown MR, Raviele NA, Prausnitz MR, Felner EI. Faster pharmacokinetics and increased patient acceptance of intradermal insulin delivery using a single hollow microneedle in children and adolescents with type 1 diabetes. Pediatr Diabetes 2013;14:459–65.

doi:10.1111/pedi.12031.

[36]   Gupta J, Park SS, Bondy B, Felner EI, Prausnitz MR. Infusion pressure and pain during

microneedle injection into skin of human subjects. Biomaterials 2011;32:6823–31.

doi:10.1016/J.BIOMATERIALS.2011.05.061.

[37]   Gill HS, Denson DD, Burris BA, Prausnitz MR. Effect of microneedle design on pain in

human volunteers. Clin J Pain 2008;24:585–94. doi:10.1097/AJP.0b013e31816778f9.

[38]   Cohen LG, Roth BJ, Nilsson J, Dang N, Panizza M, Bandinelli S, et al. Effects of coil design

on delivery of focal magnetic stimulation. Technical considerations. Electroencephalogr Clin

Neurophysiol 1990;75:350–7. doi:10.1016/0013-4694(90)90113-X.

[39]   Goldman A. Handbook of Modern Ferromagnetic Materials. Boston, MA: Springer US; 1999.

doi:10.1007/978-1-4615-4917-8.

[40]   Jayaneththi V, Aw KC, McDaid AJ. Design-based modeling of magnetically actuated soft

diaphragm materials. Smart Mater Struct 2018. doi:10.1088/1361-665x/aaacb3.

[41]   Jayaneththi VR, Aw KC, McDaid AJ. Coupled magneto-mechanical modeling of non-linear

ferromagnetic diaphragm systems. Int J Mech Sci 2019;155:360–9.

doi:10.1016/j.ijmecsci.2019.03.003.

[42]   Liu T-T, Chen K, Pan M. Experimental and modelling characterisation of adjustable hollow

Micro-needle delivery systems. Med Eng Phys 2017;49:148–56.

doi:10.1016/J.MEDENGPHY.2017.08.012.

[43]   Martanto W, Moore JS, Kashlan O, Kamath R, Wang PM, O'Neal JM, et al. Microinfusion

Using Hollow Microneedles. Pharm Res 2006;23:104–13. doi:10.1007/s11095-005-8498-8.

[44]   Martanto W, Moore JS, Couse T, Prausnitz MR. Mechanism of fluid infusion during

microneedle insertion and retraction. J Control Release 2006;112:357–61.

doi:10.1016/J.JCONREL.2006.02.017.

[45]   Wang PM, Cornwell M, Hill J, Prausnitz MR. Precise Microinjection into Skin Using Hollow Microneedles. J Invest Dermatol 2006;126:1080–7. doi:10.1038/SJ.JID.5700150.

[46]   Shrestha P, Stoeber B. Fluid absorption by skin tissue during intradermal injections through hollow microneedles. Sci Rep 2018;8:13749. doi:10.1038/s41598-018-32026-9.

[47]   Barbero AM, Frasch HF. Pig and guinea pig skin as surrogates for human in vitro penetration studies: A quantitative review. Toxicol Vitr 2009;23:1–13. doi:10.1016/J.TIV.2008.10.008.

[48]   El-Laboudi A, Oliver NS, Cass A, Johnston D. Use of Microneedle Array Devices for Continuous Glucose Monitoring: A Review. Diabetes Technol Ther 2013;15:101–15. doi:10.1089/dia.2012.0188.